Accepted by The Astronomical Journal
Preprint typeset using LaTeX style emulateapj v. 14/09/00

DOUBLE BARS, INNER DISKS, AND NUCLEAR RINGS IN EARLY-TYPE DISK GALAXIES

Peter Erwin
Instituto de Astrofisica de Canarias, C/ Via Láctea s/n, 38200 La Laguna, Tenerife, Spain
erwin@ll.iac.es

and

Linda S. Sparke
University of Wisconsin-Madison, 475 North Charter Street, Madison, WI 53706
sparke@astro.wisc.edu
Accepted by The Astronomical Journal

ABSTRACT

We present results from a survey of an unbiased sample of thirty-eight early-type (S0–Sa), low-inclination, optically barred galaxies in the field, using images both from the ground and from space. Our goal was to find and characterize central stellar and gaseous structures: secondary bars, inner disks, and nuclear rings. We find that bars inside bars are surprisingly common: at least one quarter of the sample galaxies (possibly as many as 40%) are double-barred, with no preference for Hubble type or the strength of the primary bar. A typical secondary bar is $\sim 12\%$ of the size of its primary bar and extends to 240–750 pc in radius. Secondary bars are not systematically either parallel or perpendicular to the primary; we see cases where they lead the primary bar in rotation and others where they trail, which supports the hypothesis that the two bars of a double-bar system rotate independently. We see *no* significant effect of secondary bars on nuclear activity: our double-barred galaxies are no more likely to harbor a Seyfert or LINER nucleus than our single-barred galaxies.

We find kiloparsec-scale inner disks in at least 20% of our sample; they occur almost exclusively in S0 galaxies. These disks are on average 20% the size of their host bar, and show a wider range of relative sizes than do secondary bars. Nuclear rings are present in about a third of our sample. Most of these rings are dusty, sites of current or recent star formation, or both; such rings are preferentially found in Sa galaxies. Three S0 galaxies (8% of the sample, but 15% of the S0's) appear to have purely stellar nuclear rings, with no evidence for dust or recent star formation.

The fact that these central stellar structures are so common indicates that the inner regions of early-type barred galaxies typically contain dynamically cool and disklike structures. This is especially true for S0 galaxies, where secondary bars, inner disks, and/or stellar nuclear rings are present at least two thirds of the time. If we interpret nuclear rings, secondary bars, and (possibly) inner disks and nuclear spirals as signs of inner Lindblad resonances (ILRs), then between one and two thirds of barred S0–Sa galaxies show evidence for ILRs.

Subject headings: galaxies: structure — galaxies: active —

1. INTRODUCTION

Isolated examples of multiply barred galaxies — where one or more small ("secondary") bars reside concentrically within a larger bar — have been known for over twenty-five years, the first such cases having been pointed out by de Vaucouleurs (1974). However, in the last decade high-resolution imaging has revealed numerous double-barred galaxies; see Friedli (1996) for an early review. Interest in multiply barred galaxies was stimulated by the suggestion of Shlosman, Frank, & Begelman (1989) that independently rotating, concentric bars within bars could be an important mechanism for feeding gas into the centers of galaxies, potentially fuelling nuclear activity. Subsequent n-body + hydrodynamic simulations (Friedli & Martinet 1993; Combes 1994) showed how independently rotating secondary bars might form within large-scale bars, and Maciejewski & Sparke (2000) showed that such systems could be dynamically self-consistent. Models in which the secondary bars rotate at the same speed as the primary bars have been proposed by Shaw et al. (1993) and Heller & Shlosman (1996), though the lack of preferred relative orientations in known double-barred galaxies seems to support the idea of independent rotation (Buta & Crocker 1993; Friedli & Martinet 1993; Friedli 1996).

Double- and even triple-barred galaxies continue to turn up in a variety of imaging surveys (Wozniak et al. 1995; Mulchaey, Regan, & Kundu 1997; Jungwiert et al. 1997; Martini & Pogge 1999; Márquez et al. 1999; Greusard et al. 2000; Laine et al. 2002). However, we still do not know how common such structures are in ordinary galaxies. None of the studies cited used a complete, unbiased sample; the majority were specifically focused on Seyfert galaxies and "matching" control galaxies. In addition, other substructures within large-scale bars may be confused with secondary bars. Seifert & Scorza (1996), in a study of edge-on S0 galaxies, identified several examples of inner disks, distinct from both the bulge and the outer disk, and van den Bosch & Emsellem (1998) found an edge-on S0 galaxy with both a nuclear disk and a stellar nuclear ring just outside it. Erwin & Sparke (1999) showed that stellar nuclear rings and inner disks inside the large-scale bars of mod-

erately inclined galaxies could be mistaken for secondary bars — or even coexist with them. Failure to distinguish between these structures can yield false detection rates for double bars and obscure the true diversity of structures inside bars.

In this paper we present results from a survey of a complete sample of early-type, optically barred galaxies, using the 3.5m WIYN telescope and archival optical and near-IR images from the *Hubble Space Telescope* (HST)[1], intended to find and characterize multiple bars and other central features. Erwin & Sparke (2002, hereafter Paper II) provides the details for the individual galaxies. Here, we discuss the types of structures that we found — both stellar and gaseous —, their frequencies, and their relation to other properties of the galaxies, including nuclear activity.

2. SAMPLE SELECTION AND OBSERVATIONS

Details of our sample and observations are presented in Paper II; here we give the basic outlines. We selected all barred S0–Sa galaxies in the UGC catalog (Nilson 1973) north of $-10°$ in declination, with heliocentric radial velocity ≤ 2000 km s^{-1}, major axis diameter $D_{25} \geq 2'$, and ratio of major to minor axis $a/b \leq 2$, corresponding to inclinations $\lesssim 60°$. Galaxies in the Virgo Cluster were excluded, since there is evidence that Hubble types for Virgo galaxies disagree with those for field galaxies (Koopman & Kenney 1998). The final sample had a total of 38 galaxies, listed in Table 1: twenty S0's, ten S0/a's, and eight Sa's (twenty-five of the galaxies are SB, with the remainder SAB). The median distance[2] to galaxies in the sample is 18.5 Mpc.

Because our galaxies are selected on the basis of being *optically* barred — that is, SB or SAB according to RC3 — it is possible that we missed some barred galaxies mistakenly classified as unbarred. Conflicting claims have been made about whether and how much the bar fraction increases when galaxies are observed in the near-infrared, where dust extinction is less of a problem; the most extensive survey to date is that of Eskridge et al. (2000), who classified 186 disk galaxies using H-band images. They found that the primary difference in going from RC3 optical classifications to the near-IR was the increase in the relative number of strong (SB) bars; the *total* bar fraction (SB + SAB) increases by less than 10%. Not surprisingly, this effect is weakest for early type galaxies: 65% of S0–Sab galaxies in their sample are barred according to the RC3, while 71% are barred in the near-IR. Since we restrict ourselves to S0–Sa galaxies, and select both SB and SAB classes, we are probably missing only one or two barred galaxies which were mistakenly classified as SA.

All but two of the galaxies were observed in B and R with the 3.5-m WIYN Telescope, under generally excellent seeing conditions (median seeing of $0.8''$ in R, corresponding to about 70 pc at the median distance). In addition, we found HST archival images — WFPC2 and/or NICMOS — for just over half the sample. The most common filters used were F606W and F814W with WFPC2 and F160W with NICMOS.

3. ANALYSIS AND CLASSIFICATIONS

We identify two general classes of structures inside bars: stellar and gaseous. The first class includes *secondary bars* (also called *inner bars*), *inner disks*, and *stellar nuclear rings*; see Figure 1 and Erwin & Sparke (1999) for examples. The second class includes *dusty and star-forming nuclear rings*, *nuclear spirals*, and *off-plane dust structures* (small polar rings and inclined dust disks); see Figure 2. Because our classifications are based on broad-band optical and near-IR images, we use the presence of dust and star formation (as indicated by color maps) as a proxy for the presence of gas.

A detailed discussion of our methods can be found in Paper II. To summarize briefly: we noted candidate features from ellipse fits to the R-band isophotes (for HST images, we use the reddest available filter, typically F814W for WFPC2 and F160W for NICMOS). We focused on both local peaks *and* troughs in ellipticity profiles, as well as significant deviations in position angle for the fitted ellipses (see Erwin & Sparke 1999, for an example of a secondary bar detected in NGC 3945 as a *minimum* in ellipticity, due to projection effects). The nature of individual ellipse-fit features was then checked by inspecting the images, by unsharp masking, and by the use of color maps. This let us discriminate between bars, rings, and spirals (e.g., Figure 1) — all of which can produce similar ellipse-fit features — and determine when dust extinction might be responsible. In addition, unsharp masking and color maps revealed features not immediately apparent in the ellipse fits, including some nuclear rings; color maps are a standard way of identifying and measuring dusty and star-forming nuclear rings (Buta & Crocker 1993). For off-plane dust identification, we also required kinematic evidence from the literature of misalignment between stars and gas in the galaxy.

Although it may be possible to distinguish between inner bars and disks using unsharp masks (cf. Figure 1), we use a conservative classification based on orientation: an elliptical stellar structure aligned within ten degrees of the outer disk is classified as an inner disk, unless unsharp masking shows that it is clearly a ring — compare Figure 1b and c. (While we also required that an inner disk's apparent ellipticity be less than that of the outer disk, we found no cases of *more* elliptical structures aligned with the outer disk.) Thus, we are likely to classify some inner bars with chance alignments — and possibly some poorly resolved stellar rings as well — as inner disks; the category may also include highly flattened inner bulges. However, in Section 4.2 we argue that inner disks differ statistically from inner bars, and form a genuinely distinct class.

Stellar structures such as bars, disks, and (stellar) rings can be obscured by dust. Consequently, we include the category "dusty" for galaxies where the central regions (roughly, $0.5'' \lesssim r \lesssim 10''$) are too confused by dust and/or star formation for us to determine if there is an inner *stellar* structure. This is rarely a problem where HST NIC-

[1] The WIYN Observatory is a joint facility of the University of Wisconsin-Madison, Indiana University, Yale University, and the National Optical Astronomy Observatories. Observations with the NASA/ESA Hubble Space Telescope obtained at the Space Telescope Science Institute, operated by the Association of Universities for Research in Astronomy, Inc., under NASA contract NAS5-26555.

[2] We assume $H_0 = 75$ km s^{-1} Mpc^{-1}. Distances to about one third of the galaxies are from surface-brightness fluctuation measurements; see Paper II.

MOS images are available. Intrinsically dusty structures such as nuclear spirals and dusty nuclear rings are much easier to find; we are likely to miss these only if they are too small to be properly resolved. Extremely strong Hα + [N II] emission could contaminate some R-band images; however, this usually occurs together with star formation and accompanying dust, situations where we rely on NICMOS images or else assign a "dusty" classification.

Table 1 lists the structures detected in each galaxy; Paper II provides measurements and analysis of the individual galaxies.

4. DEMOGRAPHICS OF INNER STRUCTURES

In Table 2 we list the distribution of central structures, sorted by Hubble type and bar strength. In each row, we give the fraction of all galaxies, followed by the fraction of each Hubble type or bar type, which have the specified structure; stellar structures are listed first (also including "dusty" galaxies, where we were unable to identify central stellar structures), followed by gaseous structures; as noted above, the latter are generally based on detection of dust and/or star-formation. The final section of the table groups structures by their relevance to whether or not a galaxy has an inner Lindblad resonance (see below). The most striking results are the unexpectedly high frequency of both secondary bars and inner disks, and the discordance of their distribution among Hubble types.

At least a quarter of the galaxies are multiply barred (first row of Table 2). If we assume that the "dusty" galaxies are no more or less likely to harbor secondary bars than the rest of the sample, and exclude them from the statistics, then the frequency of secondary bars may be as high as 40%. There is no obvious trend with Hubble type: Sa galaxies are as likely as S0's to be double-barred.

The fraction of galaxies with inner disks is also quite high: we find them in at least $\sim 20\%$ of the sample, or 28% of the unobscured galaxies. Since it is easier, using our techniques, to detect inner *bars* in near–face-on galaxies than it is to find inner disks, the inner-disk frequency could be as high as that of secondary bars. (Conversely, a secondary bar that is aligned with the outer disk, or an unresolved stellar nuclear ring, could be classified in error as an inner disk: at the highest level of unsharp masking, NGC 4386's inner disk bears some resemblance to a bar.) In contrast to the inner bars, inner disks show a marked preference for earlier Hubble types: all but one of the disks are found in S0's, and none at all in Sa's. The single S0/a galaxy with an inner disk is NGC 4643, and its inner disk shows some signs of being a nuclear ring rather than a disk (Paper II). In Section 4.2 we consider the question of whether inner disks are genuinely distinct from inner bars.

Nine galaxies (24% of the sample, or 36% of the unobscured galaxies) have neither an inner disk nor a secondary bar[3]. NGC 3032, NGC 4203, NGC 4665, NGC 5701, and NGC 7743 have no central structures other than (in some cases) dusty nuclear spirals, while NGC 936, NGC 2273, NGC 4245 and NGC 5377 have nuclear rings and/or spirals but no inner bars or disks.

At least eleven galaxies (29% of the sample) have nuclear rings. Eight of these rings show up in color maps as either red, blue, or a mixture of both: they are dusty and/or sites of current or recent star formation. But in NGC 936, NGC 2950, and NGC 3945, the rings appear purely stellar and are the same color as the surrounding stars; these were identified from ellipse fits and unsharp masking. The distribution of dusty and star-forming nuclear rings is clearly skewed towards the later Hubble types: the frequency is 10% for S0's versus 50% for the Sa galaxies. This is not surprising, given that Sa galaxies have more gas in the disk than S0 galaxies (e.g., Roberts & Haynes 1994).

Nine galaxies show evidence for dusty nuclear spirals (24% of the sample). The nuclear spiral in NGC 2273 includes two arms which are both blue and IR-bright, which indicates that these are star-forming sites, and the same may be true in NGC 3032. In the rest, we see no evidence for enhanced star formation, and the spirals appear to be dust structures only. As for dusty/star-forming nuclear rings, nuclear spirals are more common in later Hubble types, though the trend is not as strong.

All of the features discussed above can, with some degree of confidence, be linked with the presence of inner Lindblad resonances (ILRs) within bars. The case is strongest for nuclear rings, which are generally understood as the result of one or two ILRs acting on bar-driven gas flows. Most theoretical models of double-bar systems (Pfenniger & Norman 1990; Friedli & Martinet 1993; Shaw et al. 1993; Maciejewski & Sparke 2000) also link the presence and dynamics of a secondary bar to the primary bar's ILR(s). The case for inner disks is less clear; however, some could be mis-classified secondary bars or nuclear rings, and stars on the x_2 orbits associated with ILRs might also produce an inner disk, so we include them as well. Finally, nuclear spirals have also been linked to the influence of ILRs on bar-driven gas flows (e.g., Englmaier & Shlosman 2000; Maciejewski et al. 2002), though acoustic spirals might not depend on ILRs as directly (Elmegreen et al. 1998).

We list the possible ILR-signifiers in decreasing order of confidence in the bottom section of Table 2. If only nuclear rings are considered, then 29% of galaxies have signatures of ILRs; if secondary bars, inner disks, and nuclear spirals are also counted, this fraction becomes 66%. Thus, at least one third of our galaxies show good evidence for ILRs, and the fraction could be two thirds or even higher (since we may have missed detecting some secondary bars, inner disks, and nuclear rings). These signatures appear to be most common in the S0 galaxies. The apparent deficiency in S0/a galaxies is not statistically significant.

None of these inner structures shows any particular preference for bar strength. Within the statistical uncertainties, they are all — secondary bars, inner disks, nuclear rings, and nuclear spirals — as likely to be found in SB galaxies as in SAB galaxies.

Finally, there are six galaxies with good evidence for off-plane gas in the nuclear regions, based both on our images and kinematic evidence from the literature. Three of these were previously known or suspected (NGC 2685, NGC 4203, and NGC 7280; see discussions in Paper II for references). All but one of these candidate polar-ring galaxies are S0's — in fact, they constitute 25% of the S0's.

[3] A careful reader may notice that the percentages of inner bars, inner disks, and the lack thereof do not sum to 100% for the unobscured galaxies. This is because NGC 3945 has both an inner bar *and* an inner disk.

4.1. *Characteristics of Secondary Bars*

To investigate the orientation and sizes and of secondary bars, we deprojected their measured position angles and sizes, assuming that the bars are flat, linear structures (see Paper II for position angles and inclinations used). Figure 3 shows the relative position angles of bars in the double-barred galaxies. We used the same scheme as Buta & Crocker (1993) and Wozniak et al. (1995; hereafter W95): secondary bars can "lead" or "trail" the primary; we determine the sense of rotation from the observed spiral structure in the disk, by assuming that the spirals are trailing (Table 5 of Paper II). (The implicit assumption behind this scheme is that both bars are rotating, and that they rotate in the same direction as the trailing spiral pattern.) Counting all the bar pairs, there are eight cases where the inner bar leads the outer, and four cases where it trails. The excess of leading bars is not statistically significant; the presence of both leading and trailing secondary bars agrees with the results of Buta & Crocker, W95, and Friedli et al. (1996), and supports the idea that the two bars rotate independently of one another.

Secondary bars have a fairly limited range of sizes relative to the primary bar: they have lengths which are 0.05–0.14 times the lengths of their primary bars, with a median of 0.12 (Figure 4). Here, length refers to the deprojected upper limit on bar semi-major axis, as given in Paper II; we excluded NGC 2681, since it is unclear which of its three bars should be considered the "secondary." These figures are close to, but generally smaller than, those of W95: their double bars had a median relative size of 0.15, and a range of 0.06–0.27, if we exclude NGC 2681 and the three "B+B+B" galaxies in their sample. (These numbers do not change appreciably if we instead use the near-IR measurements from Friedli et al. 1996). Since the W95 sample was chosen on the basis of previously suspected inner features — mostly from photographic images — and was observed with lower resolution than our galaxies, there was almost certainly a selection effect in favor of large inner bars.

In linear terms, secondary bars have a median semi-major axis $a \approx 400$ pc, with the smallest being 240 pc and the largest about 1 kpc; see Figure 5. This corresponds to a range of 3% to 8% (median 5%) of the parent galaxy's R_{25} (half of the $\mu_B = 25$ diameter from RC3). This is, not surprisingly, much smaller than the R_{25}-fractional sizes of the large-scale bars in our sample (14–100%); however, some single bars in Sbc and later spirals can be this small (Martin 1995).

Figure 6 displays the maximum isophotal ellipticity measured for secondary bars versus the ellipticity of their primary bars. Secondary bars appear systematically rounder than primary bars, as found by W95. The secondary bars might be intrinsically rounder, or the isophotes could be rounder due to the superposition of light from the bright inner regions of round bulges; circularization of the isophotes due to seeing effects is another possibility. Disentangling the first two possibilities will probably require complex decomposition of the images, but we can judge the effect of seeing more simply. In Figure 7, we compare the observed ellipticity e_{max} for secondary bars and inner disks with the observed (not deprojected) length of the bar or disk divided by the full-width half-maximum (FWHM) of the image's point-spread function (PSF). The isophotal ellipticity of secondary bars and inner disks appears independent of resolution: features which are small compared with the observational resolution are not systematically rounder than large features — in fact, the secondary bars with the lowest isophotal ellipticity are among the best resolved! We conclude that the observed lower ellipticity of secondary bars reflects mostly a combination of intrinsic roundness and the superposition of bulge light; it is not due to seeing effects (Laine et al. 2002 make a similar argument).

The triple-barred galaxy NGC 2681 is a bit of a puzzle. The middle-sized secondary bar is *more* elliptical than the largest bar, which is atypical, and the length ratio of these two is 0.31 — much higher than that of any of the double bars. If we instead regard the tertiary (innermost) and secondary as a bar-within-bar system, we find a length ratio of 0.17 — larger than any of the double bars, but not dramatically so — and the tertiary is less elliptical than the secondary. The secondary-tertiary system thus appears similar to "normal" double-barred galaxies, while the primary-secondary system is anomalous.

Do secondary bars have distinct colors? In four cases (NGC 2681, NGC 2859, NGC 2962, and NGC 4314) we can identify distinct, asymmetric color features (always red) aligned or associated with the secondary. In NGC 2681, NGC 2962, and NGC 4314, the large size of the secondary bar (in NGC 2681) or HST images let us see that the color variations are clearly due to individual dust lanes, which in NGC 4314 partly resemble the classic leading-edge dust lanes found in large-scale bars and in simulations of gas flow in barred galaxies (see Figure 2; Martini et al. 2001 noted the existence of similar "leading-edge" dust lanes in the inner bars of Mrk 270 and Mrk 573). The dust lanes in NGC 4314 could also be interpreted as a nuclear spiral, which is the conservative classification we use in Table 1 and Paper II. We suspect that the red, asymmetric features aligned with the secondary bar in NGC 2859 are probably dust as well, though we lack the resolution to be sure. In four more galaxies (NGC 2950, NGC 3945, NGC 6654, and NGC 7280), there is little or no sign of color features associated with the secondary bars, other than a symmetric inward reddening trend which follows the isophotes (NGC 2950 and NGC 6654); our resolution is not high enough to tell if the innermost red regions in NGC 718 and NGC 3941 are actually aligned with their secondary bars. There is no sign in any of these galaxies that the inner bars are composed of young, blue stars. We conclude that secondary bars are probably made up of stars not too different from those of the primary bar and bulge.

We also note that several secondary bars appear relatively free of in-plane, corotating gas. In particular, NGC 2950, NGC 3945, and NGC 6654 have only a few, isolated patches of dust (or none at all), while in NGC 3941 and NGC 7280 the dust lanes and gas kinematics suggest that the gas is off-plane.

The relative sizes of these observed double-bar systems suggests that the double bars created in n-body + gas simulations are not yet good models of real double bars: the simulated inner bars are simply too large. The two inner bars formed in Friedli & Martinet's (1993) simula-

tions were 0.26 and 0.5 times the size of the outer bars, respectively; the relative size of the inner bar in Friedli et al. (1996) was 0.21. On the other hand, the double-bar system in Model IV of Rautiainen & Salo (1999) — who performed n-body simulations with *no* gas component — has a relative size[4] of ~ 0.15, which is on the upper end of the range we find.

4.2. *Inner Disks*

Are the structures that we identify as inner disks physically distinct from inner bars? Our definition (Section 3) perforce includes secondary bars which happen to have the same orientation as the outer disk, unless they are sufficiently bright and narrow to produce isophotes more elliptical than those of the outer disk. Nonetheless, there are three reasons why we believe that our inner disks form a distinct population of structures.

First, we find too many inner disks for all of them to be chance alignments of inner bars. We classify inner elliptical features as inner disks if the observed (projected) position angle is within 10° of the galaxy's line-of-nodes. At the median inclination of our galaxies (48°), this corresponds to a putative bar lying within roughly 15° of the line of nodes. By chance, then, we should expect an average of 17% of inner bars to be aligned closely enough with the outer disk for us to mis-classify them as inner disks. This would imply about two misclassified inner bars in addition to the ten that we do identify — instead, we see *eight* inner disks.

Second, inner disks show a wider range of relative sizes than do inner bars (Figure 4). They vary from $\sim 7\%$ of primary bar length to almost 40%, with a median size of 19%; the latter is well outside the range spanned by the inner bars (0.05–0.14). A Kolmogorov-Smirnov test comparing the relative sizes gives a probability of 96% that the two distributions are drawn from different parent populations. (The linear and R_{25}-fractional sizes of inner disks have more overlap with those of inner bars, though the upper bounds for inner disks are clearly higher: $a = 260$ pc to 1.7 kpc, with a median of 470 pc, or 3% to 22% of R_{25}, with a median of 7%; see Figure 5)

Third, there is the strong difference in frequency with Hubble types. All but one of the inner disks are found in S0 galaxies, while inner bars occur with equal frequency in the S0/a and Sa galaxies of our sample, and have been noted previously in galaxies as late as Sbc (e.g., Jungwiert et al. 1997).

Most of the inner disks are roughly the same color as the surrounding bar or bulge. In NGC 4143 and NGC 4643 there is evidence for nuclear spirals in the color maps, but the disks themselves are not distinct color features. The inner disks of NGC 2685 and NGC 4386, however, *are* quite distinct, and are redder than their surroundings. Both disks appear to have axisymmetric color profiles; our resolution is not good enough to tell whether this represents a gradient in stellar population, or dust obscuration.

There is one case of a secondary bar residing inside an inner disk (NGC 3945); this is also the only clear example of an inner disk coexisting with a nuclear ring. We found no cases of inner disks inside secondary bars, though these would be small structures and might have remained unresolved in our images.

4.3. *Nuclear Rings*

Nuclear rings may be more common than our detection rate of 29%, for a couple of reasons. Dusty and star-forming nuclear rings are easier to find than stellar rings, since, rather than being obscured by dust, they are often part of the dust obscuration. But a sufficiently small nuclear ring can still escape detection, at least in our ground-based images. Indeed, if we consider only those galaxies with archival HST images (just over half the sample), then the nuclear ring fraction rises to 38%. Finding *stellar* nuclear rings also requires an absence of dust *and* high signal-to-noise data (as is the case for NGC 936; see Paper II). Thus, we suspect that there are probably more stellar nuclear rings in our sample than the three we identify.

There are three galaxies with star-forming nuclear rings in our survey: NGC 2273, NGC 4245, and NGC 4314; the last is a well-studied prototype of this class of nuclear ring. Taken together, they constitute $17 \pm 9\%$ of the S0/a and Sa galaxies, a figure roughly consistent with the estimated 10% of Sc and earlier spirals thought to have circumnuclear star-forming rings, based on an HST UV imaging survey (Maoz et al. 1996, 2001). Three more galaxies have smooth, blue nuclear rings: NGC 718, NGC 2681, and the inner of NGC 5377's two nuclear rings. These may represent later stages in the star-formation process, where active star formation has mostly ceased and clumped distributions have begun to smooth out. If we lump the star-forming and blue nuclear rings together, then it appears that one-third of the S0/a–Sa galaxies have experienced circumnuclear starbursts in the last Gyr or so.

No S0 galaxies have star-forming or blue nuclear rings, and only one has a dusty nuclear ring. On the other hand, all three of the stellar nuclear rings are in S0 galaxies. This suggests that circumnuclear star formation *did* take place in at least some S0 galaxies, probably several Gyr ago. An alternate hypothesis is that the stellar rings in NGC 2950 and NGC 3945 are dynamical side-effects of their double-bar natures. Masset & Tagger (1997) showed that rings could form in n-body simulations due to the nonlinear coupling between two different pattern speeds (bar and spiral, in their simulations); such stellar rings might also form in double-barred systems if the corotation of the small bar matched the ILR of the large bar (M. Tagger, private communication). This cannot explain *all* the stellar rings, however, since NGC 936 shows no signs of an inner bar. Similarly, there is no sign of an inner bar in the Virgo SB0 NGC 4371, which has a prominent stellar nuclear ring (Erwin & Sparke 1999).

The nuclear rings we find have a range of sizes similar to, but slightly larger than, those of the inner bars (Figures 4 and 5). The median size relative to their parent bars is 11%, with a range of 3.7–30% (the upper limit is set by the large blue ring surrounding the middle bar of NGC 2681; without it, the maximum size is 22%). The linear size range is $a = 190$–1500 parsecs, with a median of 410 parsecs; the R_{25}-fractional sizes are 2.3–17% (median $= 5.3\%$ of R_{25}). All these measurements are quite consis-

[4] Measured at $t = 12.5$ Gyr from the amplitude spectra in their Figure 8, using the outermost radius of the 0.06 contours, and from the second and fifth contour levels in the particle density plots of Figure 11.

tent with those of the nuclear rings in Buta & Crocker's (1993) compilation. The median semi-major axis of their nuclear rings is 5.4% of R_{25}, with a range of 1.2–26% (using D_{25} values from RC3). They do not give bar sizes for their galaxies; but if we use the inner-ring sizes in their compilation as estimates of the bar sizes (since inner rings are typically only slightly larger than the bars they surround; Buta 1986, 1995), we can derive bar-relative sizes for their nuclear rings. This gives relative sizes of 3.7–32%, with a median of 11% — essentially identical to what we find for our nuclear rings.

Simulations of gas flow in barred galaxies (e.g., Athanassoula 1992; Shaw et al. 1993; Piner, Stone, & Teuben 1995) suggest that nuclear gas rings can lie both parallel and perpendicular to their host bars, or else at oblique angles with the major axis of the ring leading the bar (but see Heller, Shlosman, & Englmaier 2001). Is this true for our galaxies? Of the eleven rings in our sample, six appear to be leading, one is apparently perpendicular to its bar, and three are approximately circular. Only NGC 4314 has an elliptical ring which trails its (primary) bar slightly, something rarely if ever seen in any single-bar simulations. This may be due to the fact that NGC 4314 is double-barred, something we discuss below.

4.3.1. *Secondary Bars and Nuclear Rings*

As first noted by Buta & Crocker (1993) and Shaw et al. (1993), nuclear rings can coexist with secondary bars. In fact, this is rather common in our sample: six of the ten double-barred galaxies (NGC 718, NGC 2681, NGC 2859, NGC 2950, NGC 3945, and NGC 4314) have nuclear rings surrounding the secondary bars. Comparison with single-barred galaxies (excluding the dusty galaxies) shows that double-barred galaxies are far more likely to also have nuclear rings: only 27% of the single-barred galaxies have nuclear rings, versus 60% of the double-barred galaxies. On the other hand, secondary bars do not *require* nuclear rings: NGC 2692, NGC 3941, NGC 6654, and NGC 7280 all feature secondary bars without accompanying rings.

In five galaxies, we can make reasonably accurate measurements of the relative sizes of nuclear rings and secondary bars. The secondary bar in NGC 3945 is $\sim$ 65–100% of the size of the surrounding nuclear ring (the range comes from comparing the measured length of the bar to both minor and major axes of the ring); in NGC 2681 and NGC 2950, the secondary bars appear to terminate in the rings; the secondaries in NGC 2859 and NGC 4314 are $\sim$ 90% and 80% the size of their respective nuclear rings. Since nuclear rings are generally believed to mark the approximate location of a bar's inner Lindblad resonance(s) (e.g., Athanassoula 1992; Buta & Crocker 1993; Piner, Stone, & Teuben 1995), this suggests that the inner bars extend no further than their primary bars' ILRs. Pfenniger & Norman's (1990) suggestion was that a secondary bar's corotation should coincide with the primary's inner Lindblad resonance. This situation seems to hold in the simulations of Friedli & Martinet (1993) and Combes (1994), and Maciejewski & Sparke (2000) were able to construct a dynamically plausible double-bar model using a particular version of that condition. The observed sizes of secondary bars and nuclear rings are at least consistent with this ILR-CR hypothesis. The overall range of absolute and relative sizes reported above for *all* our secondary bars and nuclear rings also agrees with this: secondary bars as a class fall into the same size range as nuclear rings, though the upper limit on secondary bar size appears to be lower than that of nuclear rings.

We can also use the relative orientations of nuclear rings and secondary bars to test alternate theories of double-barred galaxies, particularly those where secondary bars are side effects of nuclear rings and corotate with the primary bar. There are no examples in our sample of *parallel* inner and outer bars separated by a nuclear ring, which is one plausible scenario (cf. NGC 4321; see Knapen et al. 2000, and references therein). However, Shaw et al. (1993) and Heller & Shlosman (1996) both produced models where a nuclear ring could induce a corotating secondary bar misaligned with the primary. The hydrodynamical + N-body simulations of Shaw et al. produced a secondary bar parallel with the elliptical, gaseous nuclear ring and leading the primary bar. Heller & Shlosman, on the other hand, found that a massive, elliptical nuclear ring (not necessarily gaseous) which led the primary bar could cause the x_1 orbits interior to the ring to twist as much as 20° in the *trailing* direction. The resulting secondary bar would then trail the primary bar and would thus *not* be aligned with the nuclear ring.

However, neither picture can explain the configurations of all of our secondary bar + nuclear ring systems. NGC 2859 *is* consistent with the model of Shaw et al. (1993) — the ring is parallel with the secondary, and both lead the primary bar by $\approx 85°$ (after deprojection); but in NGC 4314, the secondary bar and the ring are parallel but *trail* the primary by $\approx 10°$. The mechanism of Heller & Shlosman (1996) produces a trailing secondary bar, but it requires that an elliptical nuclear ring lead the primary bar by a significant amount (60°, in their example). It thus predicts that the secondary bar should be strongly *mis*aligned with the ring, which is clearly *not* true for NGC 4314. In contrast, the simulations of Friedli & Martinet (1993) produce independently rotating secondary bars with aligned, gaseous nuclear rings; this appears to be the best explanation for a system like NGC 4314 (cf. the hydrodynamical simulations of this galaxy by Ann 2001, who found that a faster-rotating inner bar produced better agreement with the observed dust lanes than a corotating inner bar). In NGC 2681 and NGC 2950, approximately *circular* nuclear rings encloses the secondary bars, which both trail (in NGC 2681) and lead (in NGC 2950) the primary bars. Again, such configurations do not agree with the corotating double-bar models.

4.4. *Nuclear Activity*

Of the 38 galaxies in our sample, we were able to find spectral classifications of their nuclei in the literature for 31; these are summarized in Table 3. Following Ho, Filippenko, & Sargent (1997a), we consider galaxies with Seyfert, LINER, and transition ("T") nuclei to be AGNs — that is, the emission-line spectra in those galaxies result at least partly from something other than star formation and associated H II regions. Those galaxies with H II or "SB" (starburst) classifications are lumped together as H II nuclei.

To compare the nuclear-activity distributions with the

results of Ho et al., we consider galaxies in the S0 and S0/a–Sab lines from their Table 2A. Combining these, we find $63 \pm 4\%$ AGNs, $15 \pm 3\%$ H II nuclei, and $22 \pm 3\%$ absorption-line nuclei, which is similar to what we see for our sample (first line of our Table 3). This is also consistent with their finding (Ho, Filippenko, & Sargent 1997b) that the frequencies of nuclear activity were similar for both barred and unbarred early-type galaxies.

Secondary bars do *not* appear to enhance — *or* reduce — nuclear activity significantly. Neither is there a significant difference when we consider galaxies with axisymmetric centers (inner disks or "none" category). Galaxies with secondary bars or inner disks may tend to lack H II nuclei, but the numbers involved are small.

Nuclear activity *is* related to the presence of a dusty/star-forming nuclear ring, a nuclear spiral, or off-plane dust near the nucleus. *None* of the galaxies with these features has an absorption-line nucleus. This is consistent with the findings of Martini & Pogge (1999): 20 of the 24 Seyfert galaxies that they studied with HST had nuclear spirals, while only 5 had nuclear-scale bars.

Bar *strength* may also be a factor: the SAB galaxies in our sample are more likely than the SB galaxies to host AGNs. While this is on the borderline of being statistically significant (at approximately the 2.5-sigma level), it does agree with the conclusions of Shlosman, Peletier, & Knapen (2000), who found, using several different samples and several measures of bar strength, that AGNs were found in galaxies with weak bars more often than in those with strong bars.

5. DISCUSSION

5.1. *Comparison with Previous Studies*

As we argued in the introduction, there have been no studies directly comparable to ours, since previous studies have looked at small samples, heterogeneous or biased samples, or focused on specific types of galaxies (such as Seyferts). Nonetheless, we would like to know if our findings — particularly the high frequencies of inner bars and disks — agree, in general, with what has been found before.

Mulchaey & Regan (1997) examined matched samples of Seyfert and control galaxies in the K band (Mulchaey, Regan, & Kundu 1997), covering a range of Hubble types from S0 to Sc. They reported that 20% of their control galaxies were double-barred, but only 10% of the Seyferts. (Considering only galaxies with at least a large-scale bar, the inner-bar fractions are $9 \pm 6\%$ and $22 \pm 10\%$, respectively.) These figures are clearly lower than our double-bar detection rate. The discrepancy becomes worse if some of their inner bars are misidentified inner disks or nuclear rings (e.g., NGC 2273; see Paper II). Using kinematic distances from LEDA, we find a median distance of 34.5 Mpc for their galaxies; combined with their median seeing of $1.0''$, this yields a typical linear resolution of 170 pc, compared with 70 pc for our ground-based images. We suspect that a number of inner bars in their galaxies may simply have been missed due to the lower resolution, a possibility they noted. Of course, there is also a difference in the samples: their galaxies were either Seyferts, or specifically chosen to match the Seyferts, and covered a wider range of Hubble types (S0–Sc).

The H-band imaging survey of Jungwiert et al. (1997) includes many more nearby galaxies; its only drawback is that it is apparently a subset of a larger, unfinished sample, with no selection criteria specified. Among their galaxies, a total of 35 barred systems meet our primary selection criteria (axis ratio < 2 and redshift < 2000 km s^{-1}), although they cover a much wider range in Hubble type (S0–Sd). The typical linear resolution was similar to that of our ground-based images: their median seeing of $1.0''$, combined with a median galaxy distance of 19 Mpc, gives a resolution of 90 pc. Although they did not have HST data, their use of H-band images does mean they were usually less affected by dust obscuration than we are. Eleven of these galaxies are identified by Jungwiert et al. as having secondary bars, for a double-bar frequency of $31 \pm 8\%$, in good agreement with what we find. Since Jungwiert et al. did not attempt to distinguish inner bars from inner disks, their double-bar frequency is in fact significantly *lower* than our combined inner-bar plus inner-disk frequency (45% of our whole sample, 64% of our unobscured galaxies). This supports our finding that the frequency of inner disks declines abruptly for Hubble types later than S0: only two of their eleven double-barred galaxies are S0.

More recently, Laine et al. (2002) used a combination of archival HST NICMOS H-band images and Digitized Sky Survey images to examine matched sets of Seyfert and "control" galaxies, similar in many respects to those of Mulchaey, Regan, & Kundu (1997). The median distance of their galaxies (31 Mpc) was quite similar, but the use of HST data means their resolution is much higher; consequently, it is not surprising that they report a higher rate of secondary bars than did Mulchaey & Regan (1997): $28 \pm 5\%$ of their barred galaxies have inner bars. As with the preceding studies, there was no attempt to distinguish inner bars from inner disks or nuclear rings, and their strict ellipse-fit criteria almost certainly means that some bars or disks were missed (e.g., NGC 4143 and NGC 7280; see Paper II). Nonetheless, the agreement with our results is good, given the broader range in Hubble type (S0–Sc; only three of their twenty multiply barred galaxies were S0's).

Seifert & Scorza (1996) looked for small-scale disks inside edge-on S0 galaxies, and found them in approximately half their sample (7 or 8 out of 15 galaxies). Since their galaxies were at roughly the same distances as ours, and since the inner disks they found have similar sizes[5], these are likely to be edge-on analogs to some of our inner structures. Although they do not report seeing conditions, the larger pixel scale of their CCDs ($0.46''$/pixel) suggests their detection efficiency could be lower than ours; they also noted that the combination of seeing and their bulge subtraction method made reliable detection of disks smaller than $5''$ in radius very difficult. Taken together, this suggests that the true inner-disk fraction for S0 galaxies may be even higher than we find.

However, Seifert & Scorza's sample almost certainly includes some barred galaxies; a number of their galaxies display the boxy or peanut-shaped bulge isophotes now known to be the signature of a bar seen edge-on (e.g., Combes et al. 1990; Kuijken & Merrifield 1995; Bureau & Freeman 1999; Lütticke, Dettmar, & Pohlen 2000). Since

[5] Measured from peaks in their a_4/a plots, which are the most appropriate match to our radii of maximum ellipticity.

we find that inner bars and disks are equally common in our barred S0 galaxies, it is possible that some of Seifert & Scorza's "inner disks" may in fact be inner bars.

In general, these previous studies appear to agree with our findings: inner bars are rather common in early-type disk galaxies, occurring in a quarter to a third of barred galaxies. Inner disks are present with a similar frequency — but restricted almost exclusively to S0 galaxies.

5.2. *Implications for the Formation and Survival of Double Bars*

The random relative alignments of inner and outer bars (Section 4.1; Buta & Crocker 1993; Wozniak et al. 1995) agrees with models where inner and outer bars rotate at different speeds, as originally argued by Buta & Crocker (1993) and Friedli & Martinet (1993). The lack of agreement between our observed inner bar + nuclear ring systems and the predictions of Shaw et al. (1993) and Heller & Shlosman (1996) is further evidence against corotating secondary bars. Thus, most double bars are likely to be independently rotating systems.

The best-known scenario for forming independently rotating double bars is essentially that of Shlosman, Frank, & Begelman (1989): a pre-existing large-scale bar drives a gas inflow into the central kiloparsec of a galaxy; once sufficient gas has accumulated, it becomes bar-unstable and a dynamically decoupled (gaseous) secondary bar forms. Friedli & Martinet (1993) and Combes (1994) demonstrated this process with n-body + hydrodynamical simulations; they showed that the stars in the inner regions of the disk could participate in the secondary bar instability, creating a secondary bar that was stellar as well as gaseous. Friedli & Benz reported that the secondary bar's corotation overlapped with the primary bar's ILR, as suggested by Pfenniger & Norman (1990). The correspondence between secondary bar sizes and nuclear ring sizes noted in Section 4.3.1 agrees with this scenario, especially if secondary bars end shortly before their own corotation.

An alternate way of creating independently rotating double-bar systems was suggested by Friedli (1996) and Davies & Hunter (1997): formation of two *counter-rotating* bars in a galaxy with counter-rotating stellar disks. Under certain conditions — specifically, with the inner part of the stellar disk counter-rotating with respect to the outer disk — a double-bar system can form, with the inner bar counter-rotating. However, the high frequency of secondary bars argues strongly against this model: Kuijken, Fisher, & Merrifield (1996) found that the fraction of S0 galaxies with significant stellar counter-rotation was quite low (less than 10%, and probably $\sim$ 1%). Thus, most double bars probably rotate independently and in the same direction.

The high frequency of secondary bars also suggests that secondary bars are either long-lived, or that they (re)form frequently. Because Friedli & Martinet (1993) found that their simulated secondary bars were rather short-lived, dissolving after only about 1–2 rotations of the outer bar ($\sim$ 250–400 Myr), it has been argued that double bars are transient (e.g., Knapen et al. 1995). Friedli & Martinet suggested that the dissolution of the secondary bar was due to bar-driven gas concentration in the center of the galaxy, in agreement with an emerging theoretical picture of bar self-destruction, where the growth of a sufficiently strong central mass concentration can disrupt a bar (Hasan & Norman 1990; Friedli & Benz 1993; Norman, Sellwood, & Hasan 1996). (In fact, in Friedli & Martinet's Model III, *both* bars dissolved at about the same time.) The conclusion from this line of reasoning, then, is that we see a high double-bar frequency because secondary bars form (and then reform after being destroyed) quite often, due to gas inflows driven by primary bars.

However, there are problems with this scenario, both theoretically and observationally. First, Combes (1994) found her inner bars lasted rather longer than Friedli & Martinet's (in some cases, more than 20 rotations of the outer bar). Second, Rautiainen & Salo (1999) reported double-bar formation in n-body simulations, *without any dissipative component*. Typically, the inner bar formed *first*, followed by the outer bar, and both were long-lived. (As pointed out in Section 4.1, the double-bar size ratio in their simulations is much closer to that of our observed double bars than the ratios of Friedli & Martinet's simulations.) And third, recent high-resolution hydrodynamic simulations by Maciejewski et al. (2002) suggest that not all inner bars drive significant gas inflows. This casts doubt on the ability of inner bars to destroy themselves as they build a central mass concentration.

If inner bars *do* form as a result of gas inflows, and are short-lived, then the prevalence of inner bars in S0 galaxies is puzzling, given that S0 galaxies are relatively gas-poor. Though some of our inner bars appear to have significant gas inside, we do see some "clean" inner bars with little or no dust (Section 4.1). The fact that inner bars are not distinctly bluer than the surrounding bulge and outer bar suggests that any star formation which might have accompanied (and consumed) the bar-forming inner gas occurred at least a Gyr ago. Finally, there are two double-barred galaxies with substantial *off-plane* gas in the nuclear regions (NGC 3941 and NGC 7280), most likely the result of accretion from other galaxies. If the inner bars in these galaxies were formed by (in-plane) gas inflow within the parent bars, then this gas probably dissipated *before* the interaction; otherwise, the infalling gas would presumably have collided with the in-plane gas and settled into the disk plane. All of this implies that the inner-bar systems we see are probably *not* recently formed by inflowing gas in the plane of the disk.

6. SUMMARY

1. In a survey of thirty-eight nearby S0–Sa barred galaxies in the field, we found a total of ten double-barred systems. We have confirmed the existence of previously reported inner bars in NGC 2681, NGC 2859, NGC 2950, and NGC 4314; NGC 2681 turns out to be *triply* barred. We have also found six new double-barred systems: NGC 718, NGC 2962, NGC 3941, NGC 3945, NGC 6654, and NGC 7280.

2. Double bar systems are surprisingly common: at least a quarter, and possibly as many as 40%, of all barred S0–Sa galaxies harbor secondary bars. These bars show no particular preference for Hubble type (within our narrow range) or primary bar strength.

3. Secondary bars are typically about 12% the size of their primary bars, with (deprojected) semi-major axes ranging from $\sim$ 250 pc to 1 kpc (3–8% of their galaxies' R_{25}). The isophotal ellipticities of secondary bars are lower than those of their parent primary bars, which may be due to intrinsic roundness, or may be an effect of being embedded within bright bulges.

4. Secondary bars probably rotate independently of, but in the same direction as, their associated primary bars. Their high frequency even in gas-poor S0 galaxies, along with the absence of significant in-plane dust in several secondary bars, suggests that they are relatively long-lived structures.

5. We also find eight inner disks inside bars. They form a statistically distinct class in terms of their size relative to the primary bar and their distribution among Hubble types; they cannot be explained as secondary bars that happen to be aligned with the galaxy's outer disk. They range in (deprojected) radius from 6% to 40% of the size of the primary bars (260 pc to 1.7 kpc). Inner disks occur almost exclusively in S0 galaxies; none were found in Sa galaxies. Since secondary bars are about as common as inner disks in S0 galaxies, it is possible that at least some of the inner disks seen in edge-on galaxies (e.g., Seifert & Scorza 1996) may actually be bars.

6. Gaseous nuclear rings, whether dusty or actively forming stars, occur predominantly in Sa galaxies (24% of the sample — but 50% of the Sa galaxies — have such nuclear rings). We found three examples of purely *stellar* nuclear rings (in the S0 galaxies NGC 936, NGC 2950, and NGC 3945), where the ring is made of stars similar in color to the surrounding bulge and bar, and dust seems to be absent; these may be the faded remnants of previous circumnuclear star formation episodes.

7. The presence or absence of secondary bars appears to have no significant effect on nuclear activity. In contrast, nuclear spirals, dusty or star-forming nuclear rings, and off-plane dust are very often accompanied by LINER or Seyfert nuclei; this agrees with the findings of Martini & Pogge (1999).

8. Counting inner bars, inner disks, and stellar nuclear rings together, at least 2/3 of all barred S0 (field) galaxies have some central stellar structure inside the bar. This may complicate disk-bulge decompositions for such galaxies, and suggests that the inner regions of early-type barred galaxies contain dynamically cool and disklike components.

We would like to thank Jay Gallagher for his help in formulating and carrying out this observational program. We also thank him and Witold Maciejewski for numerous inspirational conversations and comments on this work at various stages, and Marc Balcells and John Beckman for comments on the final version. Thanks also to Paul Martini and Isaac Shlosman for stimulating conversations, and to the referee, Eric Emsellem, for a very careful and constructive reading. The work reported here forms part of the Ph.D. thesis of Peter Erwin at the University of Wisconsin–Madison.

This research has made extensive use of the NASA/IPAC Extragalactic Database (NED) which is operated by the Jet Propulsion Laboratory, California Institute of Technology, under contract with the National Aeronautics and Space Administration. We also made use of the Lyon-Meudon Extragalactic Database (LEDA; http://leda.univ-lyon1.fr).

Finally, this research was supported by NSF grants AST 9320403 and AST 9803114, and by grant AR-0798.01-96A from the Space Telescope Science Institute, operated by the Association of Universities for Research in Astronomy, Inc., under NASA contract NAS5-26555.

REFERENCES

Ann, H. B. 2001, AJ, 121, 2515
Athanassoula, E. 1992, MNRAS, 259, 345
Bureau, M., & Freeman, K. C. 1999, AJ, 118, 126
Buta, R. 1986, ApJS, 61, 609
Buta, R., & Crocker, D. A. 1993, AJ, 105,1344
Buta, R. 1995, ApJS, 96, 39
Combes, F., Debbasch, F., Friedli, D., & Pfenniger, D. 1990, A&A, 233, 82
Combes, F. 1994, in Mass-Transfer Induced Activity in Galaxies, ed. I. Shlosman (Cambridge: Cambridge U. Press), 170
Davies, C. L., & Hunter, J. H., Jr., 1997, ApJ, 484, 79
de Vaucouleurs, G. 1974, in Formation of Galaxies, IAU Symposium No. 58, ed. J. R. Shakeshaft (Dordrecht: Reidel), 335
de Vaucouleurs, G., de Vaucouleurs, A., Corwin, H. G., Buta, R. J., Paturel, G., & Fouqué, P. 1991, Third Reference Catalogue of Bright Galaxies (New York: Springer-Verlag) (RC3)
Elmegreen, D., Elmegreen, B., Chromey, F. R., Hasselbacher, D. A., & Bissell, B. A. 1996, AJ, 111, 1880
Elmegreen,B.G., Elmegreen,D.M., Brinks,E., Yuan,C., Kaufman,M., Klaric,M., Montenegro,L., Struck,C., & Thomasson,M. 1998, ApJ, 503, L119
Englmaier, P., & Shlosman, I. 2000, ApJ, 528, 677
Erwin, P., & Sparke, L. S. 1999, ApJ, 512, L37
Erwin, P., & Sparke, L. S. 2002, in prep
Eskridge, P. B., Frogel, J. A., Pogge, R. W., Quillen, A. C., Davies, R. L., DePoy, D. L., Houdashelt, M. L., Kuchinski, L. E., Ramírez, S. V., Sellgren, K., Terndrup, D. M., & Tiede, G. P. 2000, AJ, 119, 536
Friedli, D., & Benz, W. 1993, A&A, 268, 65
Friedli, D., & Martinet, L. 1993, A&A, 277, 27
Friedli, D., Wozniak, H., Rieke, M., Martinet, L., & Bratschi, P. 1996, A&AS, 118, 461
Friedli, D. 1996, in IAU Colloquium 157: Barred Galaxies, ed. R. Buta, B. G. Elmegreen, & D. A. Crocker (San Francisco: ASP), 378
Greusard, D., Friedli, D., Wozniak, H., Martinet, L, & Martin, P. 2000, A&AS, 145, 425
Hasan, H., & Norman, C. 1990, ApJ, 361, 69
Heller, C. H., & Shlosman, I. 1996, ApJ, 471, 143
Heller, C., Shlosman, I., & Englmaier, P. 2001, ApJ, 553, 661
Ho, L. C., Filippenko, A. V., & Sargent, W. L. W. 1997a, ApJ, 487, 568
Ho, L. C., Filippenko, A. V., & Sargent, W. L. W. 1997b, ApJ, 487, 591
Jungwiert B., Combes F., & Axon, D. J. 1997, A&AS, 125, 479
Knapen, J. H., Beckman, J. E., Heller, C. H., Shlosman, I., & de Jong, R. S. 1995, ApJ, 454, 623
Knapen, J. H., Shlosman, I., Heller, C. H., Rand, R. J., Beckman, J. E., & Rozas, M. 2000, ApJ, 528, 219
Koopmann, R. A. & Kenney, J. D. P. 1998, ApJ, 497, L75

Kuijken, K., & Merrield, M. R. 1995, ApJ, 443, L13
Kuijken, K., Fisher, D., & Merrifield, M. J. 1996, MNRAS, 283, 543
Laine, S., Shlosman, I., Knapen, J. H., & Peletier, R. F. 2002, ApJ, 567, 97
Lütticke, R., Dettmar, R.-J., & Pohlen, M. 2000, A&A, 362, 435
Maciejewski, W., & Sparke, L. S. 2000, MNRAS, 313, 745
Maciejewski, W., Teuben, P. J., Sparke, L. S., & Stone, J. M. 2002, MNRAS, 329, 502
Maoz, D., Filippenko, A. V., Ho, L. C., Machetto, F. D., Rix, H., & Schneider, D. P. 1996, ApJS, 107, 215
Maoz, D., Barth, A. J., Ho, L. C., Sternberg, A., & Filippenko, A. V. 2001, AJ, 121, 3048
Márquez, I., Durret, F., González Delgado, R. M., Marrero, I., Masegosa, J. , Maza, J. , Moles, M., Pérez, E., & Roth, M. 1999, A&AS, 140, 1
Martin, P. 1995, AJ, 109, 2428
Martini, P., & Pogge, R. W. 1999, AJ, 118, 2646
Martini, P., Pogge, R. W., Ravindranath, S., & An, J. H. 2001, ApJ, 562, 139
Masset, F., & Tagger, M. 1997, A&A, 322, 442
Mulchaey, J. S., & Regan, M. W. 1999, ApJ, 482, L135
Mulchaey, J. S., Regan, M. W., & Kundu, A. 1997, ApJS, 110, 299
Nilson, P. 1973, Uppsala General Catalog of Galaxies, Uppsala Astron. Obs. Annals, 5, 1
Norman, C., Sellwood, J. A., & Hasan, H. 1996, ApJ, 462, 114
Pfenniger, D., & Norman, C. 1990, ApJ, 363, 391
Piner, B. G., Stone, J. M., & Teuben, P. J. 1995, ApJ, 449, 508
Rautiainen, P., & Salo, H. 1999, A&A, 348, 737
Roberts, M. S. & Haynes, M. P. 1994, ARA&A, 32, 115
Seifert, W., & Scorza, C. 1996, A&A, 310, 75
Shaw, M., Combes, F., Axon, D. J., & Wright, G. S. 1993, A&A, 273, 31
Shlosman, I., Frank, J., & Begelman, M. C. 1989, Nature, 338, 45
Shlosman, I., Peletier, R. F., & Knapen, J. H. 2000, ApJ, 535, L83
Shostak, G. S. 1987, A&A, 175, 4
van den Bosch, F., & Emsellem, E. 1998, MNRAS, 298, 267
Wozniak, H., Friedli, D., Martinet, L., Martin, P., & Bratschi, P. 1995, A&AS, 111, 115 (W95)

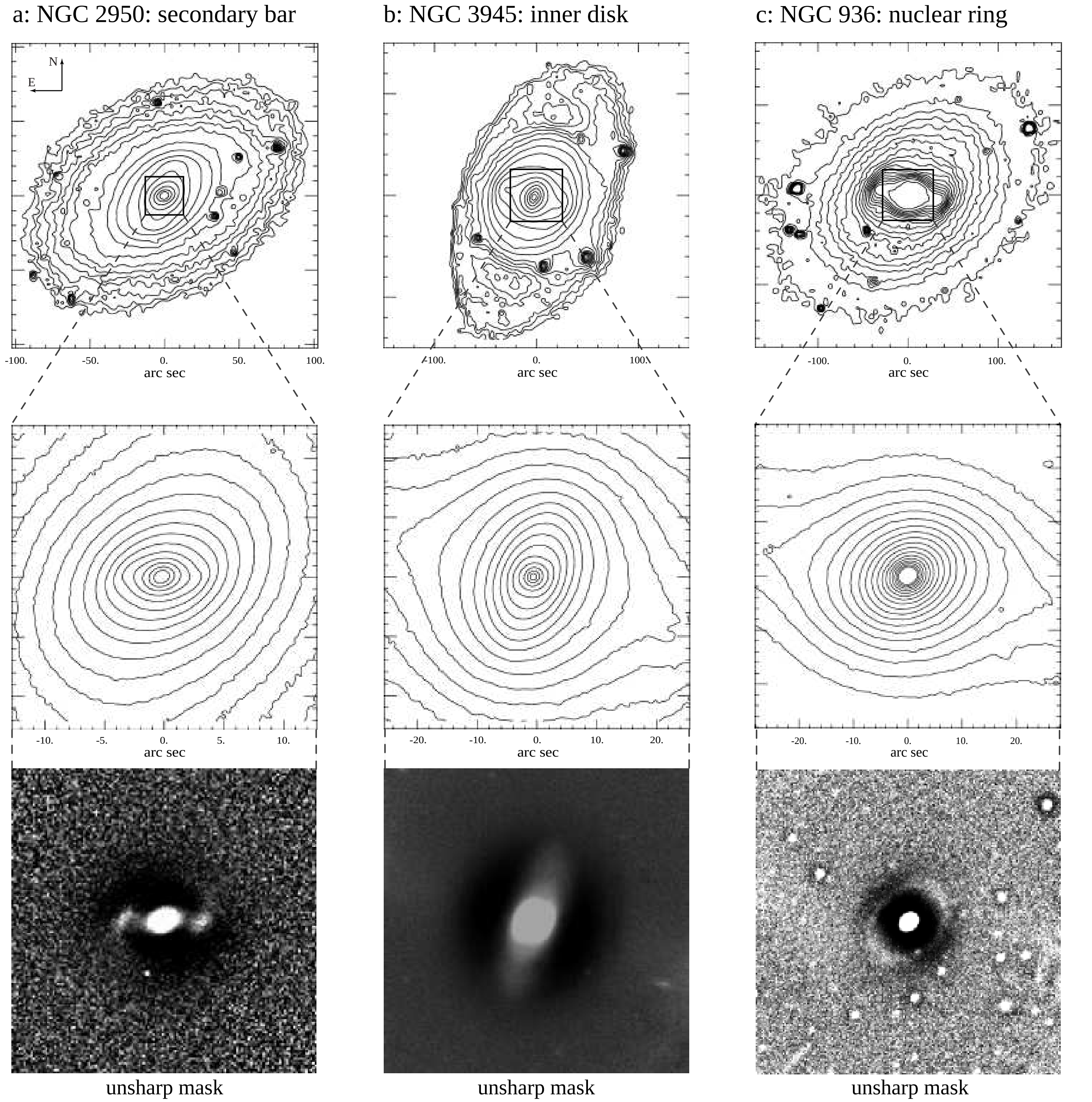

FIG. 1.— Examples of stellar structures inside the bars of three SB0 galaxies. For each galaxy, we show R-band isophotes (top and middle, except that the top part of **c** is a DSS image) and unsharp masks made from the R-band images (bottom). **a.)** Inside the primary bar of NGC 2950 is a secondary bar; the double-lobed structure in the unsharp mask is characteristic of bars. **b.)** Inside the primary bar of NGC 3945 is an inner disk — an elliptical feature at the same position angle as the galaxy's outer disk. **c.)** Inside the bar of NGC 936 is a stellar nuclear ring. As in NGC 3945, the elliptical feature is aligned with the galaxy's outer disk, but here the unsharp mask indicates a ring. *All of these structures have the same signature in ellipse fits: a peak in ellipticity at fixed position angle.* (HST images indicate that NGC 2950 also has a weak, stellar nuclear ring surrounding the secondary bar, and that NGC 3945 has both a stellar nuclear ring *and* a small secondary bar deep inside its inner disk; see Erwin & Sparke 1999 and Paper II.)

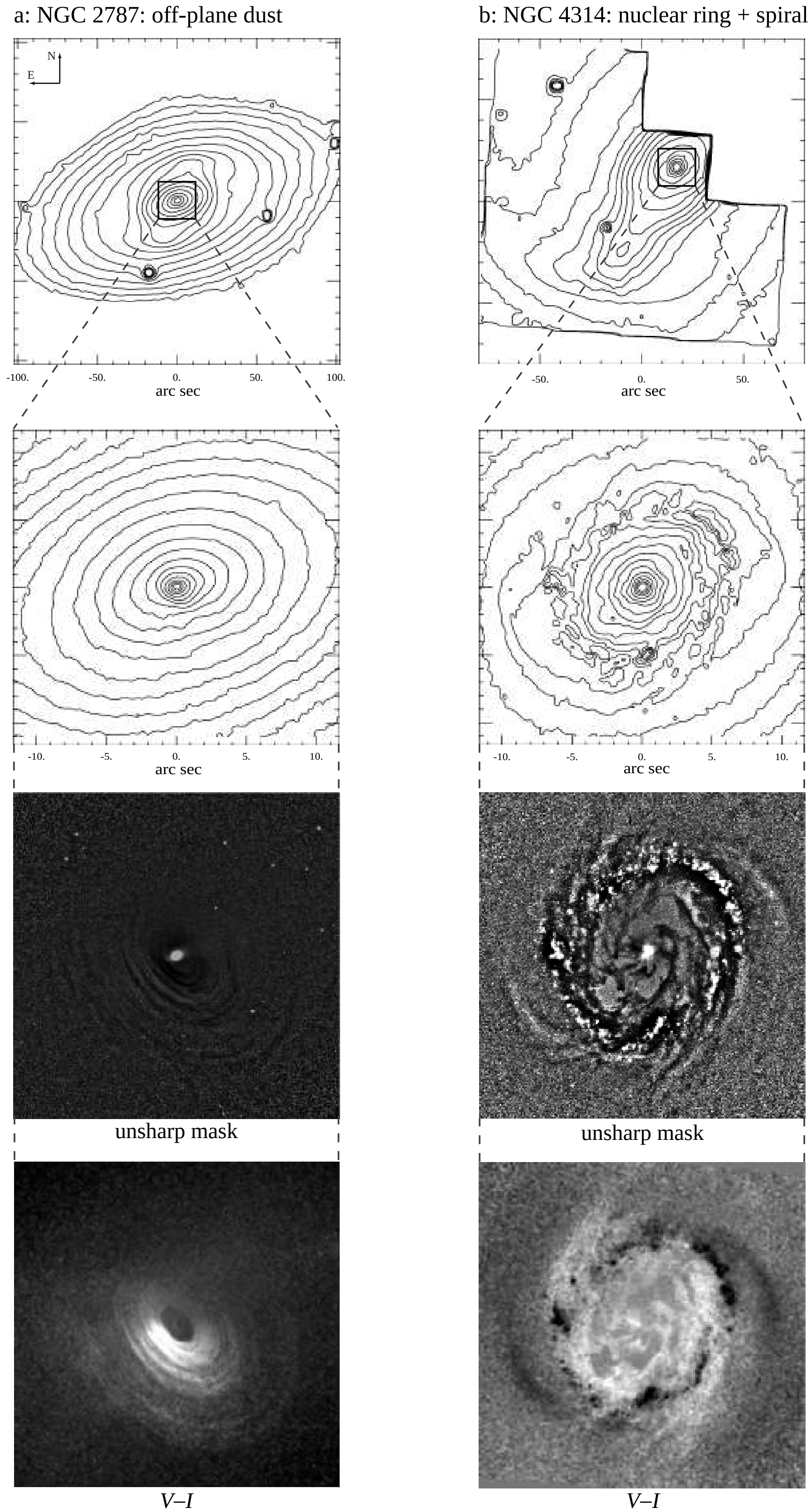

FIG. 2.— Examples of gaseous structures inside bars. We show, from top to bottom: *R*-band (top left only) and WFPC2 F814W isophotes; unsharp masks; and WFPC2 $V-I$ color maps (light = red, dark = blue). **a.)** Inside the bar of the SB0 galaxy NGC 2787 is a spectacular tilted dust disk; H I outside the optical disk is also misaligned with respect to the stars (Shostak 1987). **b.)** Inside the primary bar of the SBa galaxy NGC 4314 is a star-forming nuclear ring, with both dust lanes (red) and sites of recent star formation (blue); further inside is a dusty nuclear spiral. (We also find an inner disk outside the off-plane dust in NGC 2787, and HST near-IR images confirm a previously identified secondary bar inside NGC 4314's nuclear ring; see Paper II for details.)

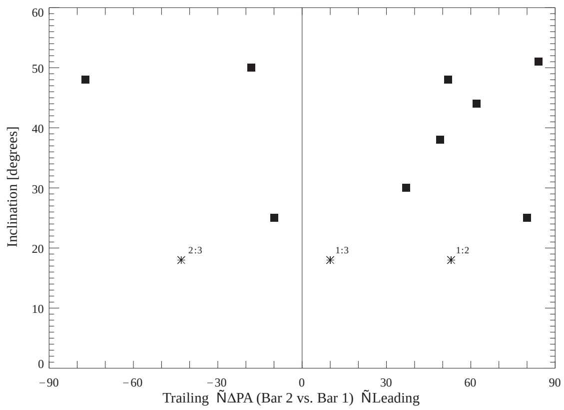

Fig. 3.— Relative position angles of secondary and primary bars, corrected for projection effects. The stars indicate the three bars of NGC 2681; the adjacent numbers indicate which of its three bars are being compared (1 = primary, 2 = secondary, 3 = tertiary).

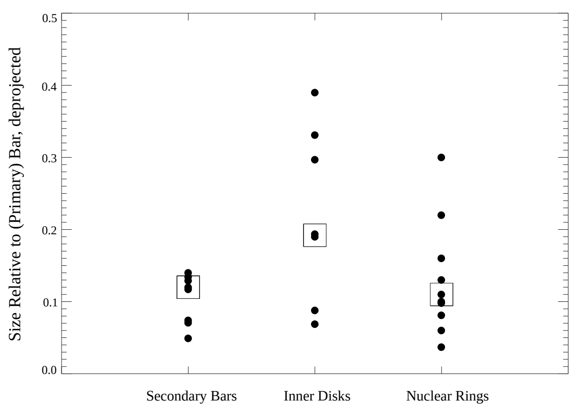

Fig. 4.— The sizes of secondary bars, inner disks, and nuclear rings, as a fraction of the host bar's length (the host bar is the galaxy's primary bar — or only bar, if it has no secondary bar). The open squares indicate the median relative size for each type of structure (excluding both inner bars of NGC 2681, for reasons given in the text).

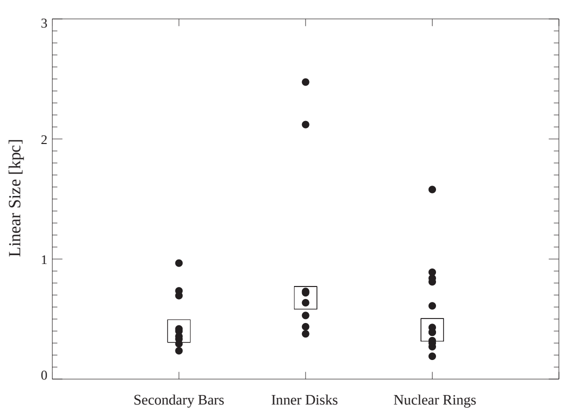

Fig. 5.— As for Figure 4, but here giving the linear sizes, in kpc, of the various inner structures. The open squares indicate the median size for each type of structure (again, excluding NGC 2681).

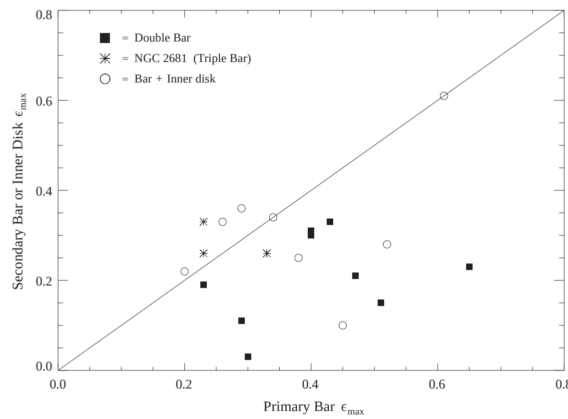

Fig. 6.— Measured isophotal (i.e., not deprojected) ellipticity of secondary bars (squares), inner disks (circles), and the multiple bars of NGC 2681 (stars) as a function of primary bar ellipticity.

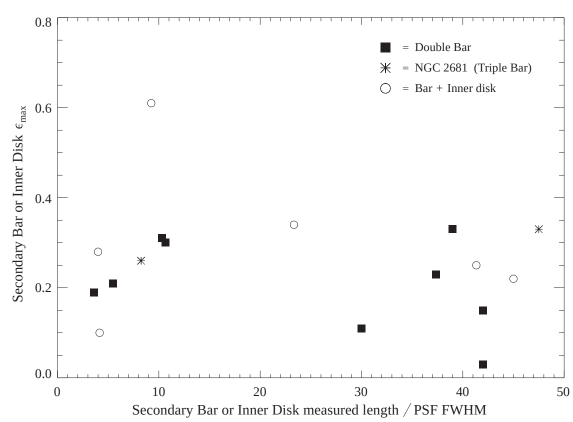

Fig. 7.— Measured isophotal ellipticity of secondary bars (secondary and tertiary bars for NGC 2681) and inner disks as a function of secondary bar or disk size, relative to the resolution of the image used to measure ellipticity (resolution defined as full-width half-maximum of point-spread function). Points farther to the right are better resolved.

Table 1
Galaxies in the WIYN Sample

Galaxy	Hubble Type (RC3)	Inner Structures
NGC 718	SAB(s)a	DB, NR
NGC 936	SB(rs)0^+	NR(s)
NGC 1022	(R′)SB(s)a	dusty
NGC 2273	(R′)SB(s)a	NS, NR
NGC 2655	SAB(s)0/a	dusty, OPG
NGC 2681	(R′)SAB(rs)0/a	DB, NR
NGC 2685	(R)SB0^+ pec	ID, OPG
NGC 2787	SB(r)0^+	dusty, ID, OPG
NGC 2859	(R)SB(r)0^+	DB, NR
NGC 2880	SB0^-	ID
NGC 2950	SB(r)0^0	DB, NR(s)
NGC 2962	(R)SAB(rs)0^+	DB
NGC 3032	SAB(rs)0^0	NS
NGC 3185	(R)SB(r)a	dusty
NGC 3412	SB(s)0^0	ID
NGC 3489	SAB(rs)0^+	dusty, NR
IC 676	(R)SB(r)0^+	dusty
NGC 3729	SB(r)a pec	dusty
NGC 3941	SB(s)0^0	DB, OPG
NGC 3945	(R)SB(rs)0^+	DB, NR(s), ID
NGC 4045	SAB(r)a	dusty
NGC 4143	SAB(s)0^0	NS, ID
NGC 4203	SAB0^-:	OPG
NGC 4245	SB(r)0/a:	NS, NR
NGC 4310	(R′)SAB0^+?	dusty
NGC 4314	SB(rs)a:	DB, NR, NS
NGC 4386	SAB0^0:	ID
NGC 4643	SB(rs)0/a	NS, ID
NGC 4665	SB(s)0/a	
NGC 4691	(R)SB(s)0/a pec	dusty
NGC 5338	SB0:	dusty
NGC 5377	(R)SB(s)a	NS, NR
NGC 5701	(R)SB(rs)0/a	NS
NGC 5750	SB(r)0/a	dusty
NGC 6654	(R′)SB(s)0/a	DB
UGC 11920	SB0/a	dusty
NGC 7280	(R)SAB(r)0^+	DB, OPG
NGC 7743	(R)SB(s)0^+	NS

Note. — Codes in the third column describe features found within the (outer) bar for each galaxy: DB = galaxy is double barred (i.e., inner/secondary bar found inside primary bar); ID = inner disk; NR = nuclear ring; NR(s) = *stellar* nuclear ring; NS = nuclear spiral; OPG = evidence for off-plane gas or dust (such as a polar ring); dusty = too dust-obscured to determine presence or absence of central stellar structures. (NGC 2787 has a large inner disk with inclined dust lanes inside; the latter obscure the central regions.)

Table 2
Central Component Frequencies by Hubble Type and Bar Strength

Component	All (38)	S0 (20)	S0/a (10)	Sa (8)	SB (25)	SAB (13)
			Stellar Structures			
Inner Bar	$26 \pm 7\%$ (10)	$30 \pm 10\%$ (6)	$20 \pm 13\%$ (2)	$25 \pm 15\%$ (2)	$24 \pm 9\%$ (6)	$31 \pm 13\%$ (4)
Inner Disk	$21 \pm 7\%$ (8)	$35 \pm 11\%$ (7)	$10 \pm 9\%$ (1)	0% (0)	$24 \pm 8\%$ (6)	$15 \pm 10\%$ (2)
No IB or ID	$24 \pm 7\%$ (9)	$20 \pm 9\%$ (4)	$30 \pm 14\%$ (3)	$25 \pm 15\%$ (2)	$24 \pm 9\%$ (6)	$23 \pm 12\%$ (3)
Nuc. Ring (s)	$8 \pm 4\%$ (3)	$15 \pm 8\%$ (3)	0% (0)	0% (0)	$12 \pm 6\%$ (3)	0% (0)
Dusty	$34 \pm 8\%$ (13)	$25 \pm 10\%$ (5)	$40 \pm 15\%$ (4)	$50 \pm 18\%$ (4)	$36 \pm 10\%$ (9)	$31 \pm 13\%$ (4)
			Gaseous Structures			
Nuc. Ring (g)	$21 \pm 7\%$ (8)	$10 \pm 7\%$ (2)	$20 \pm 13\%$ (2)	$50 \pm 18\%$ (4)	$20 \pm 8\%$ (5)	$23 \pm 12\%$ (3)
Nuc. Spiral	$24 \pm 7\%$ (9)	$15 \pm 8\%$ (3)	$30 \pm 14\%$ (3)	$38 \pm 17\%$ (3)	$28 \pm 9\%$ (7)	$15 \pm 10\%$ (2)
Off-plane Gas	$16 \pm 6\%$ (6)	$25 \pm 10\%$ (5)	$10 \pm 9\%$ (1)	0% (0)	$12 \pm 6\%$ (3)	$23 \pm 12\%$ (3)
			"ILR" features			
Nuc. Ring (all)	$29 \pm 7\%$ (11)	$25 \pm 10\%$ (5)	$20 \pm 13\%$ (2)	$50 \pm 18\%$ (4)	$32 \pm 9\%$ (8)	$23 \pm 12\%$ (3)
+ IB	$39 \pm 8\%$ (15)	$45 \pm 11\%$ (9)	$20 \pm 13\%$ (2)	$50 \pm 18\%$ (4)	$40 \pm 10\%$ (10)	$38 \pm 13\%$ (5)
+ IB, ID	$58 \pm 8\%$ (22)	$75 \pm 10\%$ (15)	$30 \pm 14\%$ (3)	$50 \pm 18\%$ (4)	$60 \pm 10\%$ (15)	$54 \pm 14\%$ (7)
+ IB, ID, NS	$66 \pm 8\%$ (25)	$85 \pm 8\%$ (17)	$40 \pm 16\%$ (4)	$50 \pm 18\%$ (4)	$68 \pm 9\%$ (17)	$62 \pm 13\%$ (8)

Note. — Percentages indicate what fraction of galaxies have a particular type of central structure, as listed in Table 1. These are not exclusive categories, since some galaxies have multiple central structures. "No IB or ID" indicates the absence of an inner/secondary bar or inner disk, though these galaxies may still have nuclear rings, spirals, or off-plane gas. "Nuc. Ring (s)" refers to stellar nuclear rings; "Nuc. Ring (g)" refers to gaseous nuclear rings, where the ring is dusty and/or shows evidence of recent star formation. "ILR" refers to features which may indicate the presence of an inner Lindblad resonance. Error bars are ± 1-σ, where σ = binomial standard deviation. Numbers in parentheses are the number of galaxies in each category (e.g., there are 20 S0 galaxies, 6 of which are double-barred).

Table 3
Nuclear Activity and Central Components

Component	AGNs	H II Nuclei	Absorption-line Nuclei
All Galaxies	$61 \pm 9\%$ (19)	$19 \pm 7\%$ (6)	$19 \pm 7\%$ (6)
SB Galaxies	$58 \pm 10\%$ (14)	$17 \pm 8\%$ (4)	$25 \pm 9\%$ (6)
SAB Galaxies	$86 \pm 13\%$ (6)	$14 \pm 13\%$ (1)	0% (0)
Inner Bar	$75 \pm 15\%$ (6)	0% (0)	$25 \pm 15\%$ (2)
Inner Disk	$60 \pm 22\%$ (3)	0% (0)	$40 \pm 22\%$ (2)
None	$56 \pm 17\%$ (5)	$22 \pm 14\%$ (2)	$22 \pm 14\%$ (2)
ID or None	$57 \pm 18\%$ (8)	$14 \pm 9\%$ (2)	$29 \pm 12\%$ (4)
Nuclear ring	$82 \pm 12\%$ (9)	$9 \pm 9\%$ (1)	$9 \pm 9\%$ (1)
Nuclear ring (g)	$88 \pm 13\%$ (7)	$13 \pm 13\%$ (1)	0% (0)
Nuclear spiral	$78 \pm 14\%$ (7)	$22 \pm 14\%$ (2)	0% (0)
Off-plane gas	100% (5)	0% (0)	0% (0)
NS or OPG	$85 \pm 10\%$ (11)	$15 \pm 10\%$ (2)	0% (0)
NR(g), NS, OPG	$89 \pm 7\%$ (17)	$11 \pm 7\%$ (2)	0% (0)

Note. — Distribution of nuclear activity for galaxies with various types of inner structure, for the 31 galaxies with classified nuclear spectra. "AGNs" = Seyfert or LINER nuclei. Percentages in each row sum to 100%, except for rounding; in parentheses are the numbers of galaxies in each set (e.g., there are 24 SB galaxies with nuclear classifications, and 14 of these — 58% — are AGNs). The first set of three rows are exclusive categories, based on the *innermost* detected structure (so NGC 3945, which has an inner bar and an inner disk, is only listed under inner bars). Error bars are 1-σ binomial errors.